

Task Allocation for Energy Optimization in Fog Computing Networks with Latency Constraints

Bartosz Kopras, Bartosz Bossy, Filip Idzikowski, Paweł Kryszkiewicz, Hanna

Bogucka

Poznan University of Technology, Poland

Abstract

This work has been submitted to the IEEE for possible publication. Copyright may be transferred without notice, after which this version may no longer be accessible.

Fog networks offer computing resources with varying capacities at different distances from end users. A Fog Node (FN) closer to the network edge may have less powerful computing resources compared to the cloud, but processing of computational tasks in an FN limits long-distance transmission. How should the tasks be distributed between fog and cloud nodes? We formulate a universal non-convex Mixed-Integer Nonlinear Programming (MINLP) problem minimizing task transmission- and processing-related energy with delay constraints to answer this question. It is transformed with Successive Convex Approximation (SCA) and decomposed using the primal and dual decomposition techniques. Two practical algorithms called Energy-EFFicient Resource Allocation (EEFFRA) and Low-Complexity (LC)-EEFFRA are proposed. They allow for successful distribution of network requests between FNs and the cloud in various scenarios significantly reducing the average energy cost and decreasing the number of computational requests with unmet delay requirements.

Index Terms

This work is funded by the Ministry of Education and Science, Poland (subvention 0312/SBAD/8159).

I. INTRODUCTION

The number of Internet of Things (IoT) devices continues to grow [1]. They often have limited memory capacity and computational power. However, processing requests of all IoT devices at a remote cloud would require an unprecedented amount of traffic traversing the Internet [2] and influencing energy consumption as well as congestion of the Internet. Moreover, some applications such as video surveillance, augmented reality, or vehicle-to-vehicle communication require low delays that cannot be fulfilled by remote cloud Data Centers (DCs). Fog computing [3] addresses these problems by introducing a fog tier (or multiple hierarchical fog tiers) between the *cloud* and the *end devices* tiers (Fig. 1)¹. It is composed of Fog Nodes (FNs) with computational and storage resources located near end users. Data transmission between *end devices* and FNs is thus faster and potentially less energy-consuming than alternative thing-to-cloud communication.

This work considers task distribution between many FNs and Cloud Nodes (CNs). We aim at minimization of network energy consumption while meeting delay constraints specific for each offloaded task. As seen in Fig. 1 an offloaded task can be processed in the node to which

¹*Fog-computing* is closely related to *edge-computing*, but we distinguish *the fog* from *the edge* by the mentioned multiple hierarchical layers of the fog and flexibility of directing the computational tasks to suitable FNs introduced by such architecture.

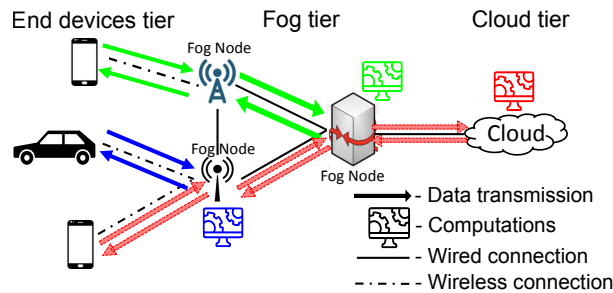


Fig. 1: Fog computing network with task offloading scenario (colors differentiate offloaded tasks).

it is originally sent (solid blue arrows), in another FN (solid green arrows), or in the cloud (hollow red arrows). A realistic network model is proposed below encompassing the energy consumption as well as the task-implementation delay, related to both the necessary computations and communication. Our model includes realistic network parameters reflecting characteristics of real-world equipment. Based on this model, we formulate the optimization problem to minimize the total (task transmission- and implementation-related) energy consumption while fulfilling total delay constraints. The optimization considers not only the assignment of tasks to the nodes but also the Central Processing Unit (CPU) frequency at each utilized node. The problem is a non-convex Mixed-Integer Nonlinear Programming (MINLP) problem, so we apply the Successive Convex Approximation (SCA) method which transforms it to a series of convex MINLP problems, and provide the optimal solution by using the primal and dual decomposition techniques and the Hungarian algorithm. A sub-optimal, lower complexity solution is also proposed. The main contributions of our work include: 1. modeling energy consumption and delays related to transmission, queuing, and computing of tasks in the fog and cloud tiers, 2. proposing and solving a complex optimization problem, 3. examining the efficiency of proposed solutions for a vast scope of network and traffic parameters. Our solutions are original in handling more complex network models, more realistic parameters, and considering both task processing- (computing-) and transmission-related energy and delay as opposed to the former and background works.

The paper is organized as follows. The overview of related work is provided in Section II. The mathematical model of the fog network is presented in Section III. Section IV defines the optimization problem, and Section V presents its solution. Simulation results for various scenarios are shown and discussed in Section VI. Section VII concludes the work.

II. RELATED WORK

We review related work while focusing on the following aspects: (i) energy consumption of fog networks related to tasks implementation (computations) and transmission of computational tasks, (ii) consideration of latency caused by both computations and transmission, (iii) fog scenarios, network and traffic models, (iv) optimization of energy consumption. The aspects (i)–(iv) stress the novelty of our work, where we jointly study communication and computing in the fog in the context of offloading of computational tasks. Works which focus on other potential applications of fog computing (e.g., content distribution/caching [4]–[6]) are therefore not included in this overview as their network and traffic scenarios are significantly different from ours. Papers not taking energy consumption into account, e.g., [7]–[9] and those who only look at power consumption as a constraint, e.g., [10] are also intentionally omitted.

The authors of [11]–[13] look at the energy consumption of individual end devices. They answer the following question: is it more efficient for an end-device to process a task locally, or to offload it to the fog/cloud? These works disregard the energy costs related to performing computations and transmission in the fog or cloud tiers of the network (our aspect (i)) and are therefore substantially different from our work. Our work and those we survey further below examine total energy consumption from the network operator point of view, tackling the following question: given a task has already been offloaded, where is it favorable to process it?

Sarkar *et al.* examine the energy consumption [14], the power consumption [15], and the task delay [14], [15] in the fog-computing network, depending on how much data is processed in the fog tier and in the cloud tier. This data is transmitted from terminal nodes. Their models include costs related to transmission, processing, and storage of data. These works show that both power/energy consumption and delay decrease with a higher percentage of tasks being processed in FNs rather than the cloud. Power/energy consumption and delay also increase with a number of terminal nodes. However, this increase is not monotonous. Moreover, a discussion

on application-specific fog computing utilization is included in [14], while costs related to the carbon footprint of the network are examined in [15].

There are multiple major differences between our work and [14], [15]. First, there is no optimization (aspect (iv)) in these works. While costs are modeled depending on where offloaded requests are sent, no solution for their optimization is proposed. Second, FNs in [14], [15] work at fixed clock-frequency while in our work, Dynamic Voltage and Frequency Scaling (DVFS) is considered (aspect (iii)). Furthermore, costs related to transmission within the fog tier (aspects (i) and (ii)) are also not considered in [14], [15]. Finally, peculiar assumptions (indefinite processing of data in cloud DCs [15], energy dissipation rate defined as a sum of energy spent over time on computations plus an average of energy spent over time on transmission [14]) and mistakes (e.g., triangle inequality used incorrectly in Sec. 5.2.1 of [15]) make results of [14], [15] biased towards showing that fog computing is significantly faster and more energy-efficient than cloud computing regardless of the offloading scenario.

In [16], offloaded requests can be served by one of the FNs or the cloud servers. Similar to our work, the objective of [16] is to minimize the power consumption of the network while maintaining delay constraints. Delay related to queuing and computing is calculated as an average response time of queuing models (M/M/1 in FNs and M/M/n in DCs). The cloud servers can adjust their clock frequency using DVFS. Results show a clear trade-off between power consumption and delay. The aspects (i), (iii), and (iv) distinguish [16] from our work. The energy/power costs are not related to data transmission in [16] (i). Also, rather than jointly optimizing energy costs related to tasks transmission and processing (computations) in the fog and the cloud, Deng *et al.* [16] heuristically split this optimization problem into three sub-problems (iv). Offloaded traffic is not divided into a number of requests, packets, or instances in [16] (iii) and is only parameterized with a single number. As a consequence, only the average delay can be calculated (and constraint satisfied), rather than the individual delay of each offloaded request. In this work, traffic offloaded from end devices consists of multiple requests, where each request

is defined with its size, arithmetic intensity, and delay requirement.

Vakilian *et al.* [17], [18] jointly optimize delay and energy consumption related to offloading in fog networks with multiple FNs. FNs can cooperate by sending workload to each other and the cloud. Similarly to [16], delay related to queuing and computing is calculated as an average response time of queuing model (M/M/1 for workload processed in FNs) with a constant value added for transmission delay between FNs. While both works use similar objective functions (weighted sum of energy consumption and delay), [18] includes *fairness coefficients* that depend on resources available to FNs while [17] does not. The authors conclude that the problem in [17] is convex. For [18], they propose a heuristic, population-based algorithm, i.e., cuckoo evolution algorithm. Results of [17] show a clear trade-off between energy consumption and delay in the network. The method proposed in [18] decreases both delay and energy consumption compared with a competing algorithm (proposed in [19]), while both works highlight that cooperation between nodes leads to lowered costs.

Vakilian *et al.* [17], [18] do not consider adjusting CPU frequencies of nodes. Furthermore, offloaded traffic is not divided into a number of requests, packets, or instances in [17], [18]. It is only parameterized with a single number (like in [16]) Hence, [17], [18] differ from our work in aspect (iii)). Finally, joint energy and latency minimization is performed in [17], [18], while energy minimization under latency constraints is performed in our work – aspect (iv).

Cai *et al.* [20] examine a network with a single task node and multiple helper nodes which lack an external power supply. The task node can process computational tasks itself or offload these tasks to the helper nodes. To do so, it needs to transfer both the task and energy required for computations to the helper node. The authors of [20] optimize cost defined as a weighted sum of delay and energy consumed by the task node for computations, energy transmission, and task transmission. The constraints include a maximum task execution delay which cannot be exceeded and offloading enough energy for computations in helper nodes. Optimization algorithms are proposed for scenarios with and without the possibility of queuing tasks.

There are multiple differences between [20] and our work. In terms of energy consumption (i) our work minimizes energy consumed by all computing nodes while [20] minimizes energy spent only by the task node, energy consumption of helper nodes is examined but only as a constraint. There are significant differences in network and traffic models (iii). [20] examines an energy harvesting scheme where helping nodes are gated by the amount of energy they receive. In [20] tasks originate from one task node while in our work they arrive from end devices at any of our FNs. Different to our work, all nodes work at fixed clock frequencies without any connection to the cloud in [20].

Power consumption and delay in fog and cloud tiers of fog computing networks are studied in [21]. Results are shown for various traffic and network parameters. A trade-off between power consumption and delay is shown both in the number of FNs and their clock frequency (more FNs and higher frequencies mean higher power consumption and lower delay). However, in [21], similarly to [15] and [14], power consumption and delay in the fog computing network is only examined – there is no energy-cost optimization (aspect (iv)). Also, while delay and energy costs related to transmission between fog and cloud tiers are considered in [21], the cost related to transmission within the fog tier is not considered (aspects (i) and (ii)).

To summarize, our work aims at minimization of energy consumed by both networking and computing equipment in the fog computing network. To the best of our knowledge, no prior work tackles the problem of jointly minimizing energy spent on both transmission and computation by distributing tasks between the fog and the cloud, while satisfying latency constraints and dynamically choosing optimal CPU clock frequencies. Finally, we take the energy- and latency-costs of inter-FN communication into account in our optimization algorithms, while in the surveyed papers these are ignored or assumed to be negligible.

III. NETWORK MODEL

We introduce the network model in this section. Notation is presented in Table I. Letters in superscript are used throughout this work as upper indices, not exponents, e.g., L^r does **not** denote L to the power of r .

In the bottom tier of the network, there are end-devices (e.g., smartphones, sensors) with some specific computational tasks. We assume that serving these tasks requires offloading them, i.e., they either cannot be processed in the end device or the end device chooses to offload them rather than process them locally. Then, they can be processed either in the fog tier, consisting of set \mathcal{F} of FNs, or in the cloud tier (set \mathcal{C} of DCs). A set of all computing nodes in the network is denoted as $\mathcal{N} = \mathcal{F} \cup \mathcal{C}$.

Unlike works that focus on end devices [11]–[13], we examine energy consumption from the point of view of the fog network. Modeling and optimizing wireless transmission is a key part of these works, e.g., allocating sub-channels to mobile devices in [12] or interference affecting transmission rates in [13]. Our system model is agnostic to the wireless technology and model/condition of the channel used for transmission between end devices and FNs. We examine requests as they appear in the fog tier of the network. Instead, we focus on the efficient distribution of offloaded tasks between fog and cloud nodes.

A. Computational Requests

Let \mathcal{T} be a numbered set $\{T_1, T_2, \dots, T_{|\mathcal{T}|}\}$ of all time instances at which computational requests arrive in the network, and have to be allocated computing resources. Let R_k be a set of all requests arriving in the network at time T_k . Each computational request $r \in R_k$ is described by the following parameters: (i) size L^r in bits, (ii) arithmetic intensity θ^r in FLOP/bit (used in FLOP/byte in [22], [23]), (iii) ratio o^r of the size of the result to the size of the offloaded task (most related works do not consider the transmission of the results [14], [15] or assume that its contribution is negligible [16], [20]; o^r equal to 1 implies the output has the same size as

the input; in case of electrocardiography signals $o^r \simeq 0.07$ [24]), (iv) FN $g^r \in \mathcal{F}$ to which the request is originally sent (before allocation)

(v) maximum tolerated delay D_{\max}^r . Let us define a binary variable a_n^r that shows where the request is computed, i.e., a_n^r equals 1 if $r \in R_k$ is computed at node $n \in \mathcal{N}$, and 0 otherwise.

B. Energy Consumption

The energy consumption model consists of two parts: communication (transmission of data) and computation (processing of data). Energy E_{cp}^r spent on processing request $r \in R_k$ equals:

$$E_{\text{cp}}^r = \sum_{n \in \mathcal{N}} a_n^r E_{\text{cp},n}^r = \sum_{n \in \mathcal{N}} a_n^r \frac{L^r \theta^r}{\beta_n}, \quad (1)$$

where $E_{\text{cp},n}^r$ is the energy spent on processing of request $r \in R_k$ at node $n \in \mathcal{N}$. β_n characterizes computational efficiency of node $n \in \mathcal{N}$ given in Floating Point Operations (FLOPs) per second per watt [25]. For cloud DCs, we assume constant CPU clock frequency f_n and efficiency β_n . For FNs, β_n depends on CPU clock frequency f_n of node $n \in \mathcal{F}$, its power consumption P_n , and number s_n of FLOPs performed within a single clock cycle of this node [26]:

$$\beta_n = \frac{f_n s_n}{P_n} = \frac{f_n s_n}{\sum_{q=0}^Q p_{n,q} f_n^q}. \quad (2)$$

We model P_n as a Q -th degree polynomial of f_n using parameters $p_{n,q}$ based on [27]. This allows the model to cover various models of CPUs. Moreover, clock frequency f_n must be within the range of minimum and maximum frequencies of the CPU installed in node $n \in \mathcal{F}$, i.e., $f_{\min,n} \leq f_n \leq f_{\max,n}$.

The energy spent on the transmission of request $r \in R_k$ equals:

$$E_{\text{comm}}^r = \sum_{n \in \mathcal{N}} a_n^r E_{\text{comm},n}^r = \sum_{n \in \mathcal{N}} a_n^r L^r (1 + o^r) \gamma_n^r, \quad (3)$$

where $E_{\text{comm},n}^r$ is the energy required to transmit (communicate) request $r \in R_k$ between FN g^r and node $n \in \mathcal{N}$ while γ_n^r is the energy-per-bit cost of transmitting data request $r \in R_k$ between

TABLE I: Notation for modelling fog computing network and defining optimization problem.

	Symbol	Description
Parameters	b_{back}	link bitrate in the backhaul and backbone network
	b_r^n	link bitrate between FNs $n \in \mathcal{F}$ and $g^r \in \mathcal{F}$
	\mathcal{C}	set of all cloud DCs
	χ	a parameter characterizing delay depending on distance
	d^n	fiberline distance from the fog to cloud DC $n \in \mathcal{C}$
	D_{max}^r	maximum tolerated delay requirement for request $r \in R_k$
	\mathcal{F}	set of all Fog Nodes
	$f_{\text{max},n}$	maximum clock frequency of node $n \in \mathcal{N}$
	$f_{\text{min},n}$	minimum clock frequency of node $n \in \mathcal{N}$
	g^r	FN to which the request $r \in R_k$ is originally sent
	γ_n^r	energy-per-bit cost of transmitting data of request $r \in R_k$ between nodes $g^r \in \mathcal{F}$ and $n \in \mathcal{N}$
	L^r	size of request $r \in R_k$
	\mathcal{N}	set of all nodes
	o^r	output-to-input data size ratio of request $r \in R_k$
	$p_{n,q}$	q -th coefficient of polynomial modeling power consumption of CPU installed in node $n \in \mathcal{N}$
	Q	degree of polynomial P_n
	R_k	set of all computational requests offloaded at T_k
	R'_k	set of rejected computational requests offloaded at T_k
	s_n	number of FLOPs performed per single clock cycle at node $n \in \mathcal{N}$
	\mathcal{T}	set of all considered time instances, when one or more computational requests arrive
	θ^r	arithmetic intensity of request $r \in R_k$
	T_k	time at which request $r \in R_k$ arrives in the network, $k \in \{1, \dots, \mathcal{T} \}$
	t_n	time at which node $n \in \mathcal{N}$ finishes computing its last task
Variables and metrics	a_n^r	whether request $r \in R_k$ is computed at node $n \in \mathcal{N}$, $a_n^r \in \{0, 1\}$
	β_n	energy efficiency (FLOPS per Watt) characterizing node $n \in \mathcal{N}$
	$D_{\text{comm},n}^r$	delay caused by transmitting request $r \in R_k$ between nodes $g^r \in \mathcal{F}$ and $n \in \mathcal{N}$
	$D_{\text{dl},n}^r$	delay caused by transmitting request $r \in R_k$ between nodes $g^r \in \mathcal{F}$ and $n \in \mathcal{N}$ – downlink
	$D_{\text{ul},n}^r$	delay caused by transmitting request $r \in R_k$ between nodes $g^r \in \mathcal{F}$ and $n \in \mathcal{N}$ – uplink
	D_{cp}^r	computational delay caused by processing request $r \in R_k$ in the network
	$D_{\text{cp},n}^r$	computational delay caused by processing request $r \in R_k$ at node $n \in \mathcal{N}$
	D_{max}^r	maximum tolerated delay requirement for request $r \in R_k$
	$D_{\text{queue},n}^r$	queuing delay of request $r \in R_k$ at node $n \in \mathcal{N}$
	D_{tot}^r	total delay of request $r \in R_k$
	$D_{\text{tot},n}^r$	total delay of processing request $r \in R_k$ at node $n \in \mathcal{N}$
	E_{comm}^r	energy spent on transmission of request $r \in R_k$
	$E_{\text{comm},n}^r$	energy cost for transmission of request $r \in R_k$ between nodes $g^r \in \mathcal{F}$ and $n \in \mathcal{N}$
	E_{cp}^r	energy spent in the network on processing request $r \in R_k$
	$E_{\text{cp},n}^r$	energy cost of processing request $r \in R_k$ at node $n \in \mathcal{N}$
	E_{tot}^r	energy spent on transmission and processing of request $r \in R_k$
	$E_{\text{tot},n}^r$	energy cost of offloading request $r \in R_k$ when computing it at node $n \in \mathcal{N}$
	f_n	clock frequency of node $n \in \mathcal{N}$
	P_n	power consumption related to computations at node $n \in \mathcal{N}$

node n and node g^r . $L^r o^r$ is the size (in bits) of results transmitted back to FN g^r . Thus, the total energy spent on offloading request $r \in R_k$ is given by:

$$E_{\text{tot}}^r = \sum_{n \in \mathcal{N}} a_n^r E_{\text{tot},n}^r = \sum_{n \in \mathcal{N}} a_n^r (E_{\text{cp},n}^r + E_{\text{comm},n}^r), \quad (4)$$

where $E_{\text{tot},n}^r$ is the energy cost of offloading request $r \in R_k$ when it is computed at node $n \in \mathcal{N}$. Energy spent on wireless transmission between end devices and FNs is not included in $E_{\text{tot},n}^r$ as we examine requests already sent by the end devices (as they appear in the FNs).

C. Delay

The delay model is divided into three parts: communication, computation, and queuing. The delay D_{cp}^r caused by computing request $r \in R_k$ equals:

$$D_{\text{cp}}^r = \sum_{n \in \mathcal{N}} a_n^r D_{\text{cp},n}^r = \sum_{n \in \mathcal{N}} a_n^r \frac{L^r \theta^r}{f_n s_n}, \quad (5)$$

where $D_{\text{cp},n}^r$ is the time required to compute request $r \in R_k$ at node $n \in \mathcal{N}$. Moreover, there are significant differences between models of communication delay for requests processed in the fog tier and the cloud tier of the network. It stems from the fact that clouds are assumed to have huge (practically infinite) computational resources with parallel-computing capabilities, and there is no need for queuing multiple requests served by the cloud DC $n \in \mathcal{C}$. They can be processed simultaneously. Meanwhile, if multiple requests are sent to the same FN $n \in \mathcal{F}$ for processing in a short time span, additional delays may occur due to congestion of computational requests (an arriving request cannot be processed until processing of all the previous requests has been completed). On the other hand, it is assumed that cloud DCs are located far away from the rest of the network (hundreds or even thousands of kilometers away) which introduces additional, transmission-related delay. Delay caused by transmitting request $r \in R_k$ between (to and from) FN $g^r \in \mathcal{F}$ and cloud node $n \in \mathcal{C}$ is equal:

$$D_{\text{comm},n}^r = \frac{L^r(1 + o^r)}{b_{\text{back}}} + d^n \cdot \chi, \quad (6)$$

where b_{back} is the link bitrate in the backhaul and backbone network, while d^n is the fiberline distance to cloud DC $n \in \mathcal{C}$. The parameter χ indicates the rate at which delay increases with distance d^n [28].

For describing delays related to transmission between FNs let us split it into the uplink (sending a request to be processed) and downlink (sending calculated results back to the origin of said request) parts denoted $D_{\text{ul},n}^r$ and $D_{\text{dl},n}^r$ respectively. For transmission between FNs, we assume delay caused by the distance between them ($d^n \cdot \chi$ in Eq. (6)) to be negligible – well below 1 ms as we use the value of $7.5\mu\text{s/km}$ for parameter χ [28] – and therefore we ignore it. The total delay caused by communication between FN $g^r \in \mathcal{F}$ and $n \in \mathcal{F}$ for request $r \in R_k$ equals:

$$D_{\text{comm},n}^r = D_{\text{ul},n}^r + D_{\text{dl},n}^r = \frac{L^r}{b_r^n} + \frac{L^r o^r}{b_r^n}, \quad (7)$$

where b_r^n is the link bitrate between FN g^r and n . As discussed earlier, when a request is sent to FN $n \in \mathcal{F}$ and there is another request being processed at this node, the request is put in a queue and waits to be processed. Let us define a scheduling variable $t_n \in \mathbb{R}^+$ which indicates when the processing of the last request scheduled at FN $n \in \mathcal{F}$ is completed.

Queuing delay of the request $r \in R_k$ at node $n \in \mathcal{F}$ is calculated as follows:

$$D_{\text{queue},n}^r = \max(0, t_n - T_k - D_{\text{ul},n}^r). \quad (8)$$

$D_{\text{queue},n}^r$ has positive values when $t_n > T_k + D_{\text{ul},n}^r$, i.e., when request r arrives at node n at time $T_k + D_{\text{ul},n}^r$ and it is queued until processing of other request(s) is completed at time t_n . For each node $n \in \mathcal{C}$ (cloud DCs), $D_{\text{queue},n}^r$ is always equal to zero, i.e., each request arriving at the cloud can immediately be processed regardless of the number of requests already being processed due to parallel processing. Thus, the total delay of processing request $r \in R_k$ is the sum of delays related to transmission, queueing, and computation:

$$D_{\text{tot}}^r = \sum_{n \in \mathcal{N}} a_n^r D_{\text{tot},n}^r = \sum_{n \in \mathcal{N}} a_n^r (D_{\text{comm},n}^r + D_{\text{queue},n}^r + D_{\text{cp},n}^r). \quad (9)$$

D. Updating Scheduling Variables in the Fog

Let us now explain how the values of scheduling variables t_n are assigned to become parameters of an optimization instance. As no requests are processed at the beginning of the simulation, we set $t_n = 0, \forall n \in \mathcal{F}$. For each $T_k \in \mathcal{T}$, after allocations a_n^r are determined, times t_n are updated according to when computation of requests offloaded to FNs is scheduled to finish:

$$t_n := \max(t_n, T_k + \sum_{r \in R_k} a_n^r (D_{ul,n}^r + D_{queue,n}^r + D_{cp,n}^r)), \forall n \in \mathcal{F}. \quad (10)$$

By using (10), each new instance of the optimization problem depends on results (allocations) of previous instances.

IV. OPTIMIZATION PROBLEM

The objective of our formulated problem is to minimize total energy spent on offloading all requests arriving at the network at time T_k , that is to find:

$$(\mathbf{a}^*, \mathbf{f}^*) = \arg \min_{\mathbf{a}, \mathbf{f}} \sum_{r \in R_k} E_{\text{tot}}^r, \quad (11)$$

subject to:

$$\sum_{n \in \mathcal{N}} a_n^r = 1 \quad \forall r \in R_k, \quad (12)$$

$$\sum_{r \in R_k} a_n^r \leq 1, \quad \forall n \in \mathcal{F}, \quad (13)$$

$$D_{\text{tot}}^r \leq D_{\text{max}}^r, \quad \forall r \in R_k, \quad (14)$$

$$f_{\min,n} \leq f_n \leq f_{\max,n} \quad \forall n \in \mathcal{F}, \quad (15)$$

$$a_n^r \in \{0, 1\}, \quad \forall r \in R_k, \forall n \in \mathcal{N}, \quad (16)$$

where $\mathbf{a}^* = \{a_n^{r*}\}$ and $\mathbf{f}^* = \{f_n^*\}$ are optimal values of the optimization variables: allocation variables a_n^r and CPU clock frequencies f_n , respectively. The constraints (12) and (13) restrict that each request must be processed at one and only one FN or cloud DC and that each FN

can process at most a single request at a time, respectively. The constraints (14) guarantee that the total delay D_{tot}^r must not be greater than the maximum acceptable one D_{max}^r . Moreover, according to the constraints (15), the CPU frequency is limited by lower and upper bound while the decision variables a_n^r take only binary values, according to constraints (16).

The optimization problem cannot be solved for some sets of requests R_k , where it is impossible to satisfy all constraints (e.g., no feasible allocation of requests so that each request is processed (12) while fulfilling its delay requirement (14)). In this case, rather than terminating the optimization without any solution (which would translate to rejecting all requests R_k), we choose to reject requests for which (14) cannot be fulfilled. The optimization is then performed over the set of remaining requests $R_k \setminus R'_k$, where R'_k denotes the set of rejected requests.

V. PROPOSED SOLUTION

The optimization problem defined in Section IV is a MINLP problem due to binary values of the allocation variables and continuous values of the CPU clock frequencies. Nonlinearity in the problem results from the power consumption model of the CPU and the set of constraints (14). Note that after substituting (2) into (1), the energy spent on processing of request $r \in R_k$ at node $n \in \mathcal{F}$ is the sum of polynomial and rational functions:

$$E_{\text{cp},n}^r = \frac{L^r \theta^r}{s_n} \left[\frac{p_{n,0}}{f_n} + \sum_{q=1}^Q p_{n,q} f_n^{q-1} \right]. \quad (17)$$

As such, for $f_n \in \mathbb{R}^+$, the convexity of (17) in f_n depends on the parameters $p_{n,q}$ (except $p_{n,1}$ and $p_{n,2}$ which have no influence on convexity, since their second derivatives are zero). If $\{p_{n,0}, p_{n,3}, \dots, p_{n,Q}\}$ are positive, the objective function is convex. If all these parameters are negative the function is concave. In these cases, standard optimization methods can be used to solve it [29]. However, if some of these parameters are negative, the others being positive, we deal with the difference of convex functions which is non-convex, requiring special optimization techniques. Therefore, in this section, the solution of the optimization problem, in the case of any possible values of CPU power consumption parameters is presented as follows.

Let us rewrite the objective function (11) with $E_{\text{cp},n}^r$ being a difference of convex functions:

$$(\mathbf{a}^*, \mathbf{f}^*) = \arg \min_{\mathbf{a}, \mathbf{f}} \sum_{r \in R_k} \sum_{n \in \mathcal{F}} a_n^r \left(\underbrace{E_{\text{cp},n}^{r+} - E_{\text{cp},n}^{r-}}_{E_{\text{cp},n}^r} + E_{\text{comm},n}^r \right), \quad (18)$$

where $E_{\text{cp},n}^{r+}$ is the sum components of $E_{\text{cp},n}^r$ with positive parameters $p_{n,q}$ and $E_{\text{cp},n}^{r-}$ is the negative of the sum components of $E_{\text{cp},n}^r$ with negative parameters $p_{n,q}$. We apply the SCA method [30]–[32] to approximate the possibly non-convex function by the series of convex ones. Since the objective function (18) is composed of differences of convex functions, the subtrahend $E_{\text{cp},n}^{r-}$ can be approximated with a linear function using the first-order Taylor series expansion at $\bar{\mathbf{f}} = \{\bar{f}_n\}$:

$$E_{\text{cp},n}^{r-}(f_n) \leq E_{\text{cp},n}^{r-}(\bar{f}_n) + \left. \frac{\partial E_{\text{cp},n}^{r-}(f_n)}{\partial f_n} \right|_{f_n=\bar{f}_n} (f_n - \bar{f}_n) \triangleq \tilde{E}_{\text{cp},n}^{r-}. \quad (19)$$

After substituting $E_{\text{cp},n}^{r-}$ with $\tilde{E}_{\text{cp},n}^{r-}$ in (18), the objective function becomes:

$$(\mathbf{a}^*, \mathbf{f}^*) = \arg \min_{\mathbf{a}, \mathbf{f}} \sum_{r \in R_k} \sum_{n \in \mathcal{F}} a_n^r \left(\underbrace{E_{\text{cp},n}^{r+} - \tilde{E}_{\text{cp},n}^{r-}}_{\tilde{E}_{\text{cp},n}^r} + E_{\text{comm},n}^r \right). \quad (20)$$

This transformed optimization problem is convex for fixed allocation variables, thus it can be solved by employing primal and dual decomposition methods [29], [33]. The primal decomposition can be applied when the problem has a coupling variable such that, when fixed to some value, the rest of the optimization problem decouples into several subproblems. Thus, let us decompose our objective problem to:

$$(\mathbf{a}^*, \mathbf{f}^*) = \arg \min_{\mathbf{a}} \arg \min_{\mathbf{f}} \sum_{r \in R_k} \sum_{n \in \mathcal{F}} a_n^r \left(\tilde{E}_{\text{cp},n}^r + E_{\text{comm},n}^r \right) \quad (21)$$

subject to (12) – (16). Now, according to (21), the solution to the optimization problem comes down to solving a two-step minimization problem. In the first step, the optimal CPU frequencies \mathbf{f}^* are determined for fixed allocation variables. First, let us define the auxiliary variables f_n^r determining the CPU frequencies of node n where request r is allocated. The relation between f_n^r and f_n is given by: $f_n = \sum_{r \in R_k} a_n^r f_n^r$ while satisfying constraints (12) and (13). The

optimal values of allocation variables \mathbf{a}^* are obtained in the second step based on the previously determined \mathbf{f}^* and constraints (12) – (13). Thus, we can now define the Lagrangian function of the subproblem for determining \mathbf{f}^* :

$$\begin{aligned} \mathcal{L}(\mathbf{a}, \mathbf{f}, \boldsymbol{\mu}, \boldsymbol{\Phi}, \boldsymbol{\Psi}) = & \sum_{r \in R_k} \sum_{n \in \mathcal{F}} a_n^r \left(\tilde{E}_{\text{cp},n}^r + E_{\text{comm},n}^r \right) + \\ & - \sum_{n \in \mathcal{F}} \Phi_n (f_{\min,n} - f_n^r) - \sum_{n \in \mathcal{F}} \Psi_n (f_n^r - f_{\max,n}) - \sum_{r \in R_k} \mu^r (D_{\text{tot}}^r - D_{\max}^r), \end{aligned} \quad (22)$$

and the Lagrange dual problem:

$$(\mathbf{a}^*, \mathbf{f}^*, \boldsymbol{\mu}^*, \boldsymbol{\Phi}^*, \boldsymbol{\Psi}^*) = \arg \min_{\boldsymbol{\mu}, \boldsymbol{\Phi}, \boldsymbol{\Psi} \geq 0} \arg \min_{\mathbf{a}} \arg \min_{\mathbf{f}} \mathcal{L}(\mathbf{a}, \mathbf{f}, \boldsymbol{\mu}, \boldsymbol{\Phi}, \boldsymbol{\Psi}) \quad (23)$$

subject to (12), (13), where $\boldsymbol{\mu} = \{\mu^r\}$, $\forall r \in R_k$, $\mu^r \in \mathbb{R}^+$, $\boldsymbol{\Phi} = \{\Phi_n\}$, $\forall n \in \mathcal{F}$, $\Phi_n \in \mathbb{R}^+$ and $\boldsymbol{\Psi} = \{\Psi_n\}$, $\forall n \in \mathcal{F}$, $\Psi_n \in \mathbb{R}^+$ are the Lagrangian multipliers responsible for fulfilling constraints (14) and (15), respectively. The dual problem in (23) can be decomposed into a master problem and subproblems, and thus solved in an iterative manner. The allocation variables \mathbf{a} and CPU frequencies \mathbf{f} are obtained by solving subproblems and then the Lagrange multipliers $\boldsymbol{\mu}, \boldsymbol{\Phi}, \boldsymbol{\Psi}$ are updated by solving the master problem for the obtained frequencies. This process continues until convergence while satisfying constraints.

A. Solving the Subproblems

The primal problem is solved in two steps. First, the optimal values of the CPU frequencies \mathbf{f}^* for each request $r \in R_k$ and node $n \in \mathcal{F}$ are obtained. Then, in the second step, the optimal values of the allocation variables \mathbf{a}^* are determined based on \mathbf{f}^* . Thus, with Karush–Kuhn–Tucker (KKT) conditions, for fixed allocation variables \mathbf{a} , we can find the optimal CPU frequencies by taking the partial derivative of (22) with respect to f_n^r setting the gradient to 0:

$$\frac{\partial \mathcal{L}}{\partial f_n^r} = 0 \quad \forall n \in \mathcal{F}, \forall r \in R_k. \quad (24)$$

Due to the polynomial form of the objective function and constraint (14), there is no closed-form solution for the above equation. Therefore, the numerical method, e.g., the Newton method with the maximum number of iterations I_{num} has to be applied to solve it.

Vector \mathbf{a}^* can be obtained based on the optimal values of the CPU clock frequency determined in the first step by solving the following optimization problem.

$$\begin{aligned} \mathbf{a}^* = \arg \max_{\mathbf{a}} & \sum_{r \in R_k} \sum_{n \in \mathcal{F}} a_n^r \left(\tilde{E}_{\text{cp},n}^{r*} + E_{\text{comm},n}^r \right) \\ & - \sum_{n \in \mathcal{F}} \Phi_n (f_{\min,n} - f_n^{r*}) - \sum_{n \in \mathcal{F}} \Psi_n (f_n^{r*} - f_{\max,n}) - \sum_{r \in R_k} \mu^r (D_{\text{tot}}^{r*} - D_{\max}^r), \end{aligned} \quad (25)$$

subject to (12), (13), where $\tilde{E}_{\text{cp},n}^{r*} = \tilde{E}_{\text{cp},n}^r (f_n^{r*})$ and $D_{\text{tot}}^{r*} = D_{\text{tot}}^r (f_n^{r*})$. The optimization problem defined in (25) is the linear assignment problem, and can be solved by the Hungarian algorithm [34]. Let us define matrix $\Theta = \{E_{\text{tot},n}^{r*}\}$, $\forall r \in R_k$ and $\forall n \in \mathcal{C}$ with $|R_k|$ rows and $|\mathcal{C}|$ columns, and matrix $\Lambda = \{\tilde{E}_{\text{tot},n}^{r*}\}$, $\forall r \in R_k$ and $\forall n \in \mathcal{F}$ with the same number of rows and $|\mathcal{F}|$ columns, where $\tilde{E}_{\text{tot},n}^{r*} = \tilde{E}_{\text{cp},n}^{r*} + E_{\text{comm},n}^r$. To reflect unlimited computational resources at each CN, we introduce matrix $\Omega = [\Lambda \Theta \otimes \mathbf{1}_{1 \times |R_k|}]$, where \otimes is the Kronecker tensor product while $\mathbf{1}_{1 \times |R_k|}$ is a vector of ones with one row and $|R_k|$ columns. It means that the columns of Θ are replicated $|R_k|$ times and matrix Ω has $|R_k|$ rows and $|R_k| \cdot |\mathcal{C}| + |\mathcal{F}|$ columns. E.g., , in the case of three tasks $|R_k| = 3$, two fog nodes $\mathcal{F} = \{1, 2\}$ and one cloud $\mathcal{C} = \{3\}$, the matrix Ω is defined as follows:

$$\Omega = \begin{bmatrix} \tilde{E}_{\text{tot},1}^{1*} & \tilde{E}_{\text{tot},2}^{1*} & E_{\text{tot},3}^{1*} & E_{\text{tot},3}^{1*} & E_{\text{tot},3}^{1*} \\ \tilde{E}_{\text{tot},1}^{2*} & \tilde{E}_{\text{tot},2}^{2*} & E_{\text{tot},3}^{2*} & E_{\text{tot},3}^{2*} & E_{\text{tot},3}^{2*} \\ \tilde{E}_{\text{tot},1}^{3*} & \tilde{E}_{\text{tot},2}^{3*} & E_{\text{tot},3}^{3*} & E_{\text{tot},3}^{3*} & E_{\text{tot},3}^{3*} \end{bmatrix} \quad (26)$$

$\underbrace{\hspace{10em}}_{E_{\text{tot},n}^{r*} \forall n \in \mathcal{F}} \quad \underbrace{\hspace{10em}}_{E_{\text{tot},n}^{r*} \forall n \in \mathcal{C}}$

Next, applying the Hungarian algorithm for matrix Ω the matrix with binary values is determined, e.g., :

$$\mathcal{H}(\Omega) = \begin{bmatrix} 0 & 1 & 0 & 0 & 0 \\ 0 & 0 & 1 & 0 & 0 \\ 0 & 0 & 0 & 0 & 1 \end{bmatrix} \quad (27)$$

The example above shows that the first task is computed in the second fog node while the second and the third task are computed in the CN. Thus, the optimal values of a_n^{r*} can be determined by:

$$a_n^{r*} = \begin{cases} \mathcal{H}(\Omega(r, n)) & \text{for } n \leq |F| \\ \sum_{j=|F|+1}^{|\mathcal{F}|+|R_k||\mathcal{C}|+1} \mathcal{H}(\Omega(r, j)) & \text{for } n > |F| \end{cases}. \quad (28)$$

B. Solving the Master Problem

We can fulfill constraints (14) and (15) by determining the search range of the optimal solution. Let $f_{\text{delay},n}^r$ denote the minimum value of f_n which satisfies the constraint (14) for request $r \in R_k$ processed at node $n \in \mathcal{F}$. These can be obtained by solving the following equation:

$$D_{\text{tot},n}^r - D_{\text{max}}^r = 0, \quad \forall n \in \mathcal{F}, \forall r \in R_k. \quad (29)$$

Inserting $D_{\text{tot},n}^r$ from Eq. (9) (together with $D_{\text{cp},n}^r$ taken from Eq. (5)) into Eq. (29) we get:

$$f_{\text{delay},n}^r = \frac{L^r \theta^r}{s_n (D_{\text{max}}^r - D_{\text{comm},n}^r - D_{\text{queue},n}^r)}. \quad (30)$$

If $f_{\text{delay},n}^r > f_{\text{max},n}$, the task r cannot be processed in FN n within the delay constraint. If $f_{\text{delay},n}^r \leq f_{\text{min},n}$, the minimum CPU clock frequency is kept at $f_{\text{min},n}$. Thus, if the obtained optimal clock frequency is in the range $f_n \in \langle \max\{f_{\text{min},n}, f_{\text{delay},n}^r\}, f_{\text{max},n} \rangle$, the Lagrange multipliers in (22) and (25) simplify by setting $\Phi_n = 0$, $\Psi_n = 0$, $\forall n \in \mathcal{F}$ and $\mu^r = 0$, $\forall r \in R_k$.

Finally, we propose the algorithm called EEFFRA (Alg. 1) for finding the solution (CPU clock frequencies and request allocation over the nodes) for total energy minimization with delay constraints, as discussed above. The computational complexity of the proposed algorithm results from the complexity of the Hungarian algorithm (line 8) and the iterative frequency finding procedure (lines 3-7). The complexity of the Hungarian algorithm is proportional to a cube of greater number: number of tasks or number of agents. In our model, the requests (tasks) can be assigned to the fog nodes or the cloud (agents). Moreover, the cloud can process more

than one request simultaneously. Therefore, in our model, we have $|R_k|$ tasks which can be assigned to the $|\mathcal{F}| + |R_k||\mathcal{C}|$ nodes, where $|R_k||\mathcal{C}|$ represents the cloud nodes which can process more than one request.

Thus, in our solution the complexity of the Hungarian algorithm equals $\mathcal{O}((|\mathcal{F}| + |R_k||\mathcal{C}|)^3)$. The second part of the computational complexity of the proposed EEFFRA algorithm results from the CPU frequency calculation. Let us observe that the CPU frequency has to be calculated for each node and each request i.e., $|R_k||\mathcal{N}|$ frequencies have to be determined. The main step of the proposed algorithm (line 4) determines the optimal CPU frequencies for a given approximation of the objective function which are then updated in the loop (line 5). This procedure is repeated until the termination conditions are met (line 7). Thus, the complexity of the CPU frequency calculation is equal to $\mathcal{O}(|R_k||\mathcal{N}|i_{\text{num}}i_{\text{sca}})$, where i_{num} and i_{sca} are the numbers of iterations of the numerical method applied to solve (24) and the SCA method, respectively. Complexity of the entire EEFFRA algorithm is therefore equal to $\mathcal{O}((|\mathcal{F}| + |R_k||\mathcal{C}|)^3 + |R_k||\mathcal{N}|i_{\text{num}}i_{\text{sca}})$.

Algorithm 1 The EEFFRA in the fog computing networks.

- 1: **Inputs:** $L^r, \theta^r, o^r, D_{\max}^r$ for $r \in R_k$, $\{p_{n,0}, p_{n,3}, \dots, p_{n,Q}\}$, $f_{\min,n}, f_{\max,n}, s_n, d^n$ for $n \in \mathcal{F}$, γ_n^r , b_r^n for $r \in R_k$ and $n \in \mathcal{F}$ and b_{back}, χ , maximum number of iterations $I_{\text{num}}, I_{\text{sca}}$, iteration index i_{sca} , maximum error ε and initial values of optimization variables $\bar{\mathbf{f}}$
 - 2: **Outputs:** $E_{\text{tot},n}^r$ for $r \in R_k$ and $n \in \mathcal{F}$, $\mathbf{f}^*, \mathbf{a}^*$
 - 3: **repeat**
 - 4: calculate \mathbf{f}^* by solving (24) in the range $f_n \in \langle \max\{f_{\min,n}, f_{\text{delay},n}^r\}, f_{\max,n} \rangle$ for $\Phi_n = 0$, $\Psi_n = 0, \forall n \in \mathcal{F}$ and $\mu^r = 0, \forall r \in R_k$ using numerical method with max. I_{num} iterations
 - 5: $\bar{\mathbf{f}} \leftarrow \mathbf{f}^*$
 - 6: $i_{\text{sca}} \leftarrow i_{\text{sca}} + 1$
 - 7: **until** $|\bar{\mathbf{f}} - \mathbf{f}| \leq \varepsilon$ **or** $i_{\text{sca}} = I_{\text{sca}}$
 - 8: calculate \mathbf{a}^* using the Hungarian method for the matrix Ω and (28)
 - 9: $E_{\text{tot},n}^r \leftarrow \tilde{E}_{\text{tot},n}^r$ for $r \in R_k$ and $n \in \mathcal{F}$
-

C. Low-complexity solution (LC-EEFFRA)

In the following approach to our optimization problem called Low-Complexity EEFFRA (LC-EEFFRA), we remove the Hungarian algorithm from EEFFRA leading to reduced computational complexity to $\mathcal{O}(|R_k| |\mathcal{N}| i_{\text{num}} i_{\text{sca}})$. The optimal values of frequency \mathbf{f}^* are determined in the same way as in Alg. 1 while the values of \mathbf{a}^* are obtained in a heuristic manner. In this heuristic approach, only a single request $r \in R_k$ is considered at a time. It is allocated to node n^* where the energy consumption for processing r is the lowest, i.e., we find:

$$n^* = \arg \min_n E_{\text{tot},n}^r \forall r \in R_k. \quad (31)$$

Values t_n are updated after allocation of each request to prevent multiple collisions of two or more requests at the same FN. The examination order of requests arriving at the same time is random to emulate a decentralized approach.

VI. RESULTS

Results obtained from computer simulations are presented in this section. Let us consider a network with $|\mathcal{F}| = 10$ FNs and $|\mathcal{C}| = 1$ cloud DC. Simulation parameters are summarized in Table II. The process of generating requests for simulations is as follows. At time $T_k \in \mathcal{T}$ there appear between 5 and 10 (uniform distribution) new computational requests. The value T_k is generated at a random delay after previous time instance T_{k-1} . The difference $T_k - T_{k-1}$ is chosen to be a random variable of exponential distribution with average value 50 ms (intensity = 20 s⁻¹). The requests have randomly (with uniform distribution) assigned values of their parameters (size, arithmetic intensity, delay requirement) in ranges shown in Table II.

It is assumed that each FN uses a single Intel Core i5-2500K as its CPU. Data relating frequency, voltage, and power consumption of i5-2500K is taken from [35] and fit into Eq. (2) adopted from [27]. The resulting power consumption and energy efficiency are plotted in Fig. 2. These figures show that power consumption increases faster-than-linearly with operating frequency and that the frequency with the highest energy efficiency is around 2.6 GHz. The cloud

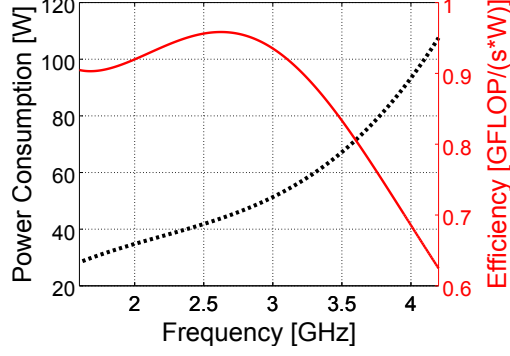


Fig. 2: Power consumption and energy efficiency of Intel Core i5-2500K vs. CPU frequency.

CPUs are parameterized according to the *Intel Xeon Phi* family commonly used in computer clusters [25], [36] characterized with $s = 32$ FLOP/cycle [26], and run at a constant frequency 1.5 GHz. Transmission parameters are analogous to those used in [21]. If not stated differently, simulations for each data point are obtained over 550 time instances T_k . Results from the first 50 instances are discarded. Random number generator seeds are kept the same for each value of swept parameters for a fair comparison of results.

Our solutions, i.e., EEFFRA and LC-EEFFRA, are compared with three reference methods. The first method, called *Cloud Only*, processes all requests in the cloud. The second method, called *Fog Only*, processes all requests in the FNs. The FNs' CPU frequencies and requests-to-nodes assignments are determined using LC-EEFFRA. Finally, the third method, called *Fog Simple*, processes requests in the same FN that these requests arrived at. Still, it uses optimal FNs' CPU frequencies determined using LC-EEFFRA. Simulations are performed using MATLAB.

A. Convergence of Algorithms and Optimality of Solution

EEFFRA utilizes SCA for finding optimal operating frequencies and the Hungarian algorithm for assigning requests to nodes. The Hungarian algorithm is guaranteed to find the optimum in polynomial time [34]. SCA is guaranteed to converge [39]. To show the SCA convergence rate, we plot normalized energy costs resulting from offloading requests depending on the maximum number of algorithm iterations in Fig. 3. Apart from SCA iterations I_{sca} , we also vary the

TABLE II: Simulation parameters.

Symbol	Value/Range	Symbol	Value/Range	Symbol	Value/Range
Requests, $r \in R_k$					
L^r	[1,10] MB	θ^r	[1,100] FLOP/bit	o^r	[0, 0.5]
D_{\max}^r	[100, 1000] ms	$ R_k $	[5,10]	$\overline{T_k} - \overline{T_{k-1}}$	50 ms
Number of nodes					
$ \mathcal{F} $	10	$ \mathcal{C} $	1		
Computations in the fog [26], [27], [35], $n \in \mathcal{F}$					
s_n	16 FLOP/cycle	$p_{n,3}, p_{n,2}$	5.222, 34.256	$f_{\min,n}$	1.6 GHz
Q	3	$p_{n,1}, p_{n,0}$	88.594, -47.152	$f_{\max,n}$	4.2 GHz
Computations in the cloud [25], [26], $n \in \mathcal{C}$					
f_n	1.5 GHz	s_n	32 FLOP/cycle		
Transmission [28], [37], [38]					
$d^n, n \in \mathcal{C}$	2000 km	χ	7.5 $\mu\text{s/km}$	b_{back}	1 Gbps
$b_r^n, n \in \mathcal{F}$	1 Gbps	$\gamma_n^r, n \in \mathcal{F}$	0.3 nJ/(bit-hop)	$\gamma_n^r, n \in \mathcal{C}$	10 nJ/bit

maximum number of iterations I_{num} used to find the optimum CPU frequencies in Alg. 1. For clarity of convergence analysis, we assume that there is no cloud, i.e., $|\mathcal{C}| = 0$. The operating frequency of the cloud is not adjusted (not a variable) and therefore does not influence the analysis. Normalization is obtained by plotting the relative difference between the cost achieved by EEFFRA and the optimal cost found by solving the original problem without SCA. Since the degree of polynomial modeling CPU power consumption in these simulations equals 3, the optimal frequencies f_n^{r*} can be found analytically for each request $r \in R_k$ and node $n \in \mathcal{F}$ which result in the lowest cost $E_{\text{cp},n}^r$ while fulfilling (14). Since the first derivative of $E_{\text{cp},n}^r$ over f_n from (17) is continuous everywhere except at singularity at $f_n = 0$, and has at most 3 real roots, the optimal frequency $f_n \in \langle \max \{f_{\min,n}, f_{\text{delay},n}^r\}, f_{\max,n} \rangle$ is either obtained for the endpoint of this interval or for one of the roots of $\frac{d}{df_n} E_{\text{cp},n}^r(f_n)$. The lowest value $E_{\text{cp},n}^r$ for these frequencies determines the optimal frequency f_n^{r*} . The solution is continued as described in Section V from Eq. (25). It is visible in Fig. 3 that EEFFRA converges both quickly and to values close to the optimal ones.

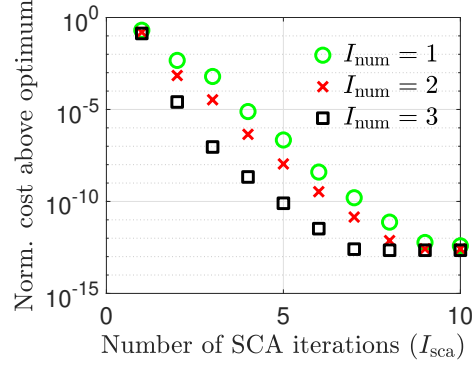


Fig. 3: Convergence of solutions found by EEFFRA to optimum with number of iterations.

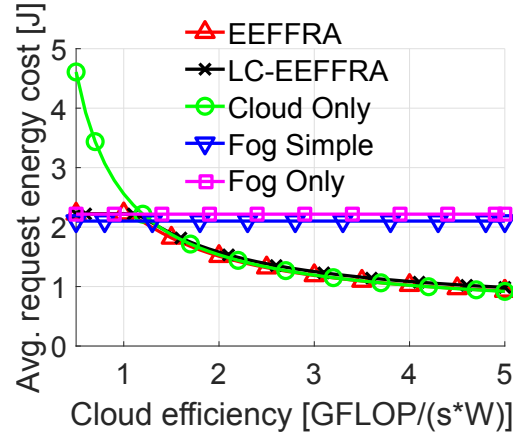


Fig. 4: Influence of cloud energy efficiency on average energy cost for chosen policies.

B. Impact of Computational Energy Efficiency of the Cloud

First, we vary the values of the computational efficiency of the cloud DC in the range $[0.5, 5.0]$ GFLOP/(s·W) (median value for 500 of the most powerful commercially available computer clusters is 2.962 GFLOP/(s·W) [25]). The average energy costs per successfully processed request are shown in Fig. 4. At low computational efficiency of the cloud, policies utilizing only nodes in the fog tier (*Fog Simple*, *Fog Only*) perform similarly to those utilizing both the fog and the cloud. *Cloud only* approach has the highest energy consumption at low efficiency of the cloud (up to around 1.3 GFLOP/(s·W)). Above that level *Cloud only* is characterized with lower energy consumption than *Fog Simple* and *Fog Only* solutions and similar to EEFFRA and LC-EEFFRA solutions as under these parameters it is the most efficient to process most

requests in the cloud. EEFFRA is slightly more efficient than LC-EEFFRA at higher cloud efficiency values. The percentage of requests which were unable to be processed using each of the offloading policies is the following: The *Fog Simple* solution where FNs cannot “share” computational requests between themselves has the highest ratio of rejected requests (8.2%) , while only 1.4%-1.7% requests (percentage varies depending on cloud efficiency – lower for higher efficiency) are rejected by both proposed solutions utilizing both fog and cloud (EEFFRA and LC-EEFFRA). *Fog Only* and *Cloud Only* have rejection rates of 1.9% and 4.3% respectively. Requests which are rejected tend to have larger sizes and higher arithmetic intensities (as shown later in Figs. 5b and 8). It “artificially” decreases the average-per-request cost of methods with higher rejection rates in Fig. 4, e.g., causing *Fog Simple* to show lower average cost than *Fog Only*).

Let us examine more closely where EEFFRA chooses to offload computational requests and what parameters impact these decisions. Fig. 5 shows histograms of parameters characterizing offloaded requests obtained after running simulations for 2000 T_k instances. Fig. 5a and Fig. 5b show the probabilities of requests being processed in the fog tier of the network and those rejected due to too low delay requirement at cloud efficiency of 1.3 GFLOP/(s·W). A similar histogram for requests processed in the cloud would be superfluous as probabilities for results processed in the fog, in the cloud, and those rejected sum to 1. Unsurprisingly, Fig. 5b shows that results with strict latency requirements are less likely to be successfully processed in time. In Fig. 5a up to 40% of high arithmetical intensity tasks with delay requirements of around 200 ms are processed in the fog tier as a result of the cloud being unable to fulfill these requirements. In Fig. 5a one can see a “threshold” between 40 and 50 FLOP/bit below which requests are chosen by EEFFRA to be served by the FNs rather than the cloud. Similar histograms plotted for other values of cloud efficiencies show that this threshold increases with a less efficient cloud and decreases with a more efficient cloud. In particular, for efficiencies below 1.0 GFLOP/(s·W), all requests are processed in Fog. On the other hand, even for infinitely high efficiencies of the

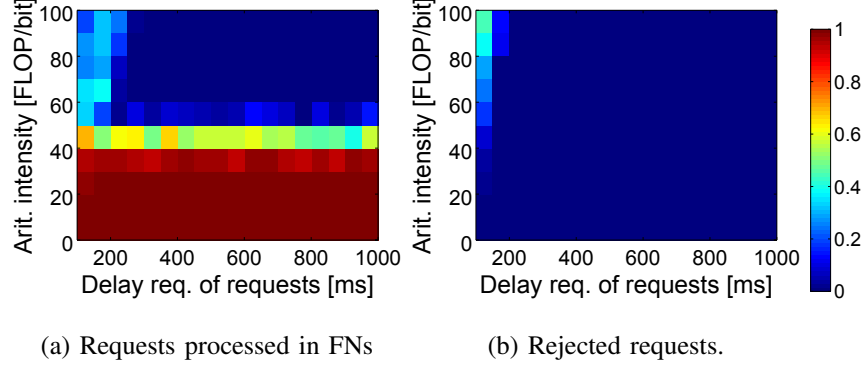


Fig. 5: Histograms of requests at 1.3 GFLOP/(s·W) cloud efficiency. Results of EEFRA.

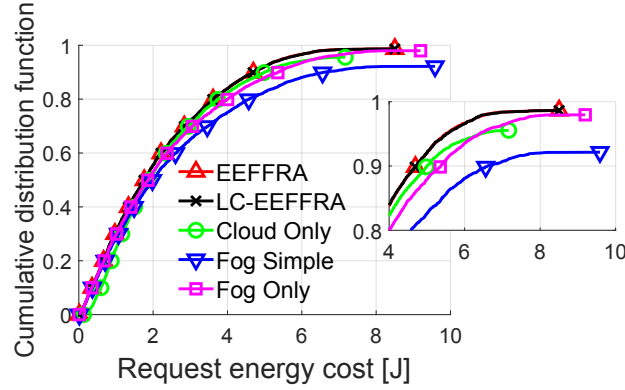


Fig. 6: Cumulative Distribution Functions (CDFs) of request processing energy cost at cloud efficiency of 1.3 GFLOP/(s·W). Comparison of different policies.

cloud around 20% of tasks remain processed in the fog tier (low-intensity ones for which the cost of transmission to the cloud outweighs computational costs in the fog and those with strict delay requirements). up to 40% of high arithmetical intensity tasks with delay requirements of around 200 ms are processed in the fog tier as a result of the cloud being unable to fulfill these requirements.

To better illustrate differences in requests allocation policies, we plot CDF of energy cost spent on a single request. Energy spent on rejected requests is assumed to be infinite for the purpose of CDF plots. Such results can be seen in Fig. 6. First, it is visible that utilization of both fog and cloud tiers of the network yields significantly better results than utilizing nodes in

only one tier. The proposed EEEFFRA and LC-EEFFRA provide the lowest required energy cost for each percentile of the CDFs. All methods do not reach 1 on the y-axis, i.e., some requests cannot be processed within a given delay budget. Our methods achieve the lowest rejection rate as shown in the inset of Fig. 6.

C. Impact of Delay Requirements and Size of Requests on the Offloading Decisions

Let us see how the energy consumption and the percentage of rejected requests change with the size and the delay requirement of computation requests. The energy efficiency of the cloud is set to 1.3 GFLOP/(s·W) and parameter sweeps for other parameters are performed. All other parameters are generated according to Table II.

Fig. 7 plots CDFs of energy consumption costs of processing single requests with delay requirements: 100 ms (Fig. 7a) and 200 ms (Fig. 7b). At the required delay of 100 ms, all methods have high rejection rates, with *Cloud Only* being clearly the worst-suited for low-latency applications. The differences between the rest of the methods are minor – the requests with such low delay requirements either can or cannot be solved in time at the receiving FN and the ability of nodes to transmit tasks between themselves does not improve performance. With a 200 ms, the differences between approaches become more profound. Utilizing both fog and cloud (EEFFRA, LC-EEFFRA) gives the lowest rejection rates and energy costs. *Fog Simple* meanwhile has the worst performance.

Fig. 8 plots CDFs of energy consumption costs of processing single requests with sizes 5 MB, (Fig. 8a) and 10 MB (Fig. 8b). EEEFFRA, LC-EEFFRA, and *Cloud Only* show the highest energy efficiency for 5 MB requests. However, *Cloud Only* fails to process a small number of requests within a given delay requirement, while *Fog Only*, EEEFFRA, and LC-EEFFRA process all requests successfully. Fig. 8c shows that EEEFFRA and LC-EEFFRA achieve the lowest energy costs and rejection rates for 10 MB requests. It is worth observing that for both request sizes *Cloud Only* has the highest energy costs up to at least 20-th percentile (caused by energy spent

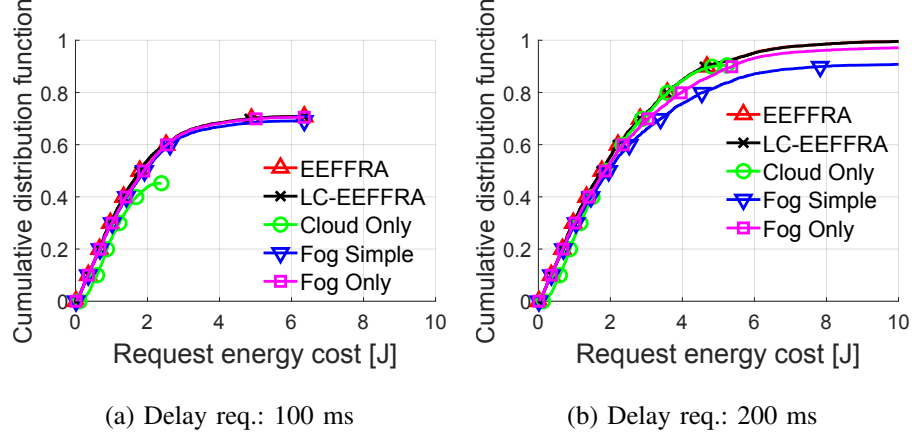


Fig. 7: CDFs of request processing energy cost – influence of delay requirement of requests.

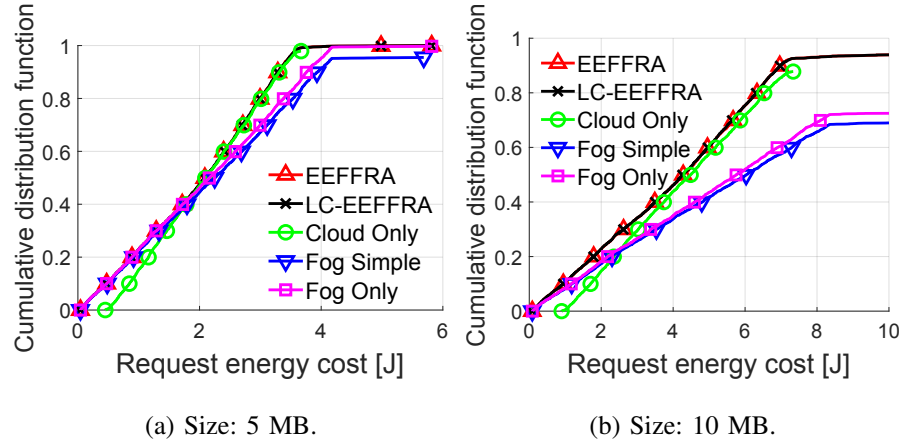


Fig. 8: CDFs of request processing energy cost – influence of size of requests.

for transmission), but for higher percentiles (influenced by requests with higher arithmetical intensities) its costs are lower than that of either *Fog Only* or *Fog Simple*.

D. Impact of CPU Frequency of Fog Nodes

In previous sections, it was assumed that FNs can dynamically adjust their operating frequency (and voltage) to minimize energy consumption while satisfying delay requirements. Let us assume that all FNs utilize the same, fixed CPU frequency. Fig. 9 shows the average energy cost and percentage of rejected requests plotted as a function of this fixed frequency (swept between 1.6 and 4.2 GHz with a 0.1 GHz step). Results for *Cloud Only* are constant as no requests are processed in FNs. *Fog Simple* and *Fog Only* methods have high rejection rates at low frequencies.

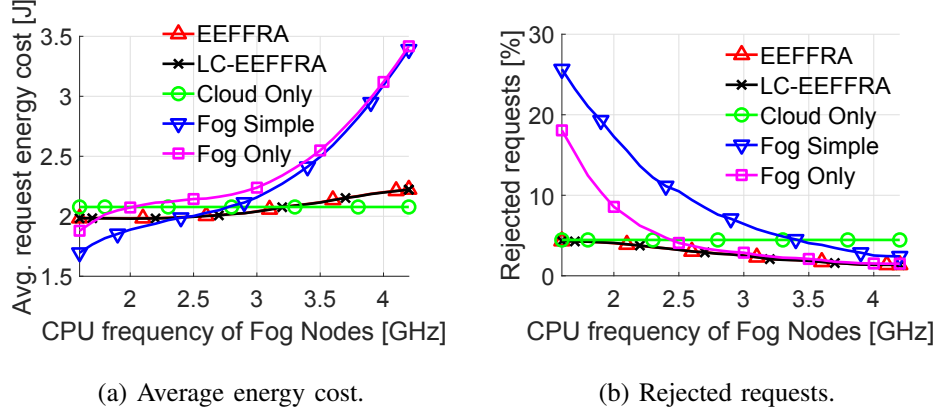


Fig. 9: Influence of fixed CPU frequency of FNs.

Meanwhile EEFFRA and LC-EEFFRA have the lowest rejection rates while also having the lowest (considering the rejected requests are not taken into account by this metric) energy costs. As the frequency of FNs increases the rejection rates decline and average energy cost increases for all methods utilizing FNs. However, this effect is considerably smaller for EEFFRA and LC-EEFFRA (utilizing resources in both fog and cloud tiers) than for *Fog Simple* and *Fog Only*.

Let us compare the efficiency of the network employing EEFFRA with and without DVFS. As shown in Fig. 9 the possibility to send requests to the cloud diminishes the impact of FNs' operating frequency on energy costs and rejection rate. Therefore, to focus on the differences, Fig. 10 shows the results of simulations for a network with 10 FNs and no connection to the cloud. We compare CDFs of energy costs per request achieved utilizing DVFS with the following fixed frequencies of FNs: 1.6 GHz (minimum), 2.6063 GHz (optimal frequency for maximizing energy efficiency as seen in Fig. 2, later referred to as 2.6 GHz), and 4.2 GHz (maximum). The range of possible arithmetic intensities of requests is increased to $[1, 500]$ to make the requests highly variable in terms of required computations speed while the mean time between sets of requests is increased ($\overline{T_k} - \overline{T_{k-1}} = 500$ ms). Rejection rates are increasing with decreasing fixed FN frequency. On the other hand, 4.2 GHz has the highest energy cost. EEFFRA utilizing DVFS manages to maintain the lowest energy cost for every percentile.

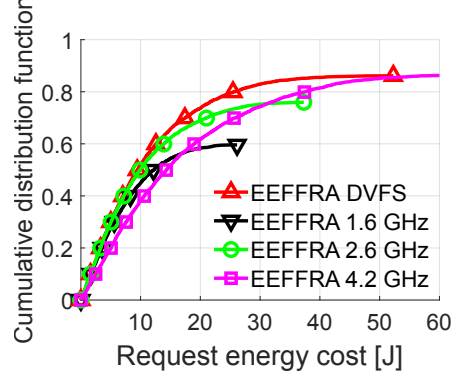


Fig. 10: CDFs of request processing energy cost – comparison of FNs working at fixed frequencies and utilizing DVFS. Parameters: $\overline{T_k} - T_{k-1} = 500$ ms, $\theta^r \in [1, 500]$ FLOP/bit.

VII. CONCLUSION

We have formulated the optimization problem of minimizing the energy consumption in the fog computing network while maintaining the latency constraints. This energy consumption is assumed to be resulting from both transmission and processing of offloaded computational tasks (computation requests originating from the end-users). The latency and energy consumption models and their parameters are based on real-life computing and networking equipment product data sheets and measurements. The proposed EEEFRA algorithm solves the proposed optimization problem using its successive approximations for adjusting clock frequencies of CPUs in fog nodes. A sub-optimal, lower complexity solution LC-EEEFRA, which does not require coordinated decision making, is also proposed. Results of simulations show that both EEEFRA and LC-EEEFRA can significantly reduce average energy cost and the number of rejected computational requests by distributing the workload between fog and cloud nodes. The proposed solutions can be seen as promising alternatives for managing fog computing networks.

REFERENCES

- [1] P. Cerwall *et al.*, “Ericsson mobility report,” Ericsson, Tech. Rep., 2018.
- [2] Cisco, “Cisco global cloud index: Forecast and methodology, 2016–2021 white paper,” Cisco, Tech. Rep., 2018.

- [3] F. Bonomi, R. Milito, J. Zhu, and S. Addepalli, "Fog computing and its role in the Internet of Things," in *Proc. of the Mobile Cloud Computing (MCC) Workshop*, Aug. 2012.
- [4] D. Chen, S. Schedler, and V. Kuehn, "Backhaul traffic balancing and dynamic content-centric clustering for the downlink of fog radio access network," in *2016 IEEE 17th International Workshop on Signal Processing Advances in Wireless Communications (SPAWC)*, July 2016.
- [5] J. Xu, K. Ota, and M. Dong, "Saving energy on the edge: In-memory caching for multi-tier heterogeneous networks," *IEEE Communications Magazine*, vol. 56, no. 5, pp. 102–107, 2018.
- [6] K. Wang, J. Li, Y. Yang, W. Chen, and L. Hanzo, "Energy-efficient multi-tier caching and node association in heterogeneous fog networks," in *2020 IEEE 92nd Vehicular Technology Conference (VTC2020-Fall)*, 2020, pp. 1–5.
- [7] Z. Liu, Y. Yang, K. Wang, Z. Shao, and J. Zhang, "Post: Parallel offloading of splittable tasks in heterogeneous fog networks," *IEEE Internet of Things Journal*, vol. 7, no. 4, pp. 3170–3183, 2020.
- [8] M. K. Hussein and M. H. Mousa, "Efficient task offloading for IoT-based applications in fog computing using ant colony optimization," *IEEE Access*, vol. 8, pp. 37 191–37 201, 2020.
- [9] L.-A. Phan, D.-T. Nguyen, M. Lee, D.-H. Park, and T. Kim, "Dynamic fog-to-fog offloading in SDN-based fog computing systems," *Future Generation Computer Systems*, vol. 117, pp. 486–497, 2021.
- [10] R. Lin, Z. Zhou, S. Luo, Y. Xiao, X. Wang, S. Wang, and M. Zukerman, "Distributed optimization for computation offloading in edge computing," *IEEE Transactions on Wireless Communications*, vol. 19, no. 12, pp. 8179–8194, 2020.
- [11] T. Q. Dinh, J. Tang, Q. D. La, and T. Q. S. Quek, "Offloading in mobile edge computing: Task allocation and computational frequency scaling," *IEEE Transactions on Communications*, vol. 65, no. 8, pp. 3571–3584, 2017.
- [12] C. You, K. Huang, H. Chae, and B. H. Kim, "Energy-efficient resource allocation for mobile-edge computation offloading," *IEEE Transactions on Wireless Communications*, vol. 16, no. 3, pp. 1397–1411, 2017.
- [13] L. Liu, Z. Chang, and X. Guo, "Socially aware dynamic computation offloading scheme for fog computing system with energy harvesting devices," *IEEE Internet of Things Journal*, vol. 5, no. 3, pp. 1869–1879, 2018.
- [14] S. Sarkar and S. Misra, "Theoretical modelling of fog computing: a green computing paradigm to support IoT applications," *IET Networks*, vol. 5, no. 2, pp. 23–29, Mar. 2016.
- [15] S. Sarkar, S. Chatterjee, and S. Misra, "Assessment of the suitability of fog computing in the context of Internet of Things," *IEEE Transactions on Cloud Computing*, vol. 6, no. 1, pp. 46–59, 2018.
- [16] R. Deng, R. Lu, C. Lai, T. H. Luan, and H. Liang, "Optimal workload allocation in fog-cloud computing toward balanced delay and power consumption," *IEEE Internet Things Journal*, vol. 3, no. 6, pp. 1171–1181, 2016.
- [17] S. Vakilian and A. Fanian, "Enhancing users' quality of experienced with minimum energy consumption by fog nodes cooperation in internet of things," in *2020 28th Iranian Conference on Electrical Engineering (ICEE)*, 2020, pp. 1–5.
- [18] S. Vakilian, S. V. Moravvej, and A. Fanian, "Using the cuckoo algorithm to optimizing the response time and energy consumption cost of fog nodes by considering collaboration in the fog layer," in *2021 5th International Conference on Internet of Things and Applications (IoT)*, 2021, pp. 1–5.
- [19] Y. Dong, S. Guo, J. Liu, and Y. Yang, "Energy-efficient fair cooperation fog computing in mobile edge networks for smart city," *IEEE Internet of Things Journal*, vol. 6, no. 5, pp. 7543–7554, 2019.
- [20] P. Cai, F. Yang, J. Wang, X. Wu, Y. Yang, and X. Luo, "Jote: Joint offloading of tasks and energy in fog-enabled IoT networks," *IEEE Internet of Things Journal*, vol. 7, no. 4, pp. 3067–3082, 2020.
- [21] B. Koprass, F. Idzikowski, and P. Kryszkiewicz, "Power consumption and delay in wired parts of fog computing networks," in *2019 IEEE Sustainability through ICT Summit (StICT)*, Montreal, Canada, Jun. 2019.
- [22] Y. Wang, T. Zhao, L. Li, Z. Hou, and J. Gu, "Roofline model based performance-aware energy management for scientific computing," in *2018 9th International Symposium on Parallel Architectures, Algorithms and Programming (PAAP)*, 2018.
- [23] N. M. Allayla and S. A. Dawwd, "Performance optimization on GPGPU & multicore CPU using roofline model," *IOP Conference Series: Materials Science and Engineering*, vol. 1152, no. 1, May 2021.
- [24] T. N. Gia, M. Jiang, A. Rahmani, T. Westerlund, P. Liljeberg, and H. Tenhunen, "Fog computing in healthcare Internet of Things: A case study on ECG feature extraction," in *Proc. WNM*, Oct. 2015.
- [25] E. Strohmaier, J. Dongarra, H. Simon, and M. Martin, "Green500 list for November 2020," last accessed on 02.12.2021. [Online]. Available: <https://www.top500.org/lists/green500/2020/11/>
- [26] R. Dolbeau, "Theoretical peak FLOPS per instruction set: a tutorial," *The Journal of Supercomputing*, vol. 74, no. 3, 2018.
- [27] S. Park, J. Park, D. Shin, Y. Wang, Q. Xie, M. Pedram, and N. Chang, "Accurate modeling of the delay and energy overhead of dynamic voltage and frequency scaling in modern microprocessors," *IEEE Transactions on Computer-Aided Design of Integrated Circuits and Systems*, vol. 32, no. 5, pp. 695–708, 2013.

- [28] M. Olbrich, F. Nadoln, F. Idzikowski, and H. Woesner, “Measurements of path characteristics in PlanetLab,” TU Berlin, Tech. Rep. TKN-09-005, July 2009.
- [29] S. Boyd and L. Vandenberghe, *Convex Optimization*. Cambridge University Press, 2004.
- [30] B. Bossy, P. Kryszkiewicz, and H. Bogucka, “Energy efficient wireless relay networks with computational awareness,” *IEEE Transactions on Communications*, vol. 68, no. 2, pp. 825–840, 2020.
- [31] —, “Energy efficient resource allocation in multiuser DF relay interference networks,” in *2018 IEEE Globecom Workshops (GC Wkshps)*, Dec. 2018.
- [32] T. Wang and L. Vandendorpe, “Successive convex approximation based methods for dynamic spectrum management,” in *Proc. IEEE ICC*, Jun. 2012.
- [33] D. P. Palomar and Mung Chiang, “A tutorial on decomposition methods for network utility maximization,” *IEEE Journal on Selected Areas in Communications*, vol. 24, no. 8, pp. 1439–1451, 2006.
- [34] H. W. Kuhn, “The Hungarian method for the assignment problem,” *Naval Research Logistics Quarterly*, vol. 2, no. 1-2, pp. 83–97, 1955.
- [35] H. Wong, “A comparison of Intel’s 32nm and 22nm Core i5 CPUs: Power, voltage, temperature, and frequency,” Oct. 2012, last accessed on 02.12.2021. [Online]. Available: <http://blog.stuffedcow.net/2012/10/intel32nm-22nm-core-i5-comparison/>
- [36] Intel, “Intel delivers new architecture for discovery with intel xeon phi coprocessor,” Nov. 2012, last accessed on 02.12.2021. [Online]. Available: <https://newsroom.intel.com/news-releases/intel-delivers-new-architecture-for-discovery-with-intel-xeon-phi-coprocessors/#gs.721jg4jg>
- [37] P. Bertoldi, “EU code of conduct on energy consumption of broadband equipment: Version 6,” 2017.
- [38] W. Van Heddeghem, F. Idzikowski, W. Vereecken, D. Colle, M. Pickavet, and P. Demeester, “Power consumption modeling in optical multilayer networks,” *Photonic Network Communications*, vol. 24, no. 2, pp. 86–102, 2012.
- [39] A. Zappone, E. Björnson, L. Sanguinetti, and E. Jorswieck, “Globally optimal energy-efficient power control and receiver design in wireless networks,” *IEEE Transactions on Signal Processing*, vol. 65, no. 11, pp. 2844–2859, June 2017.